PHYSICAL REVIEW B **90**, 060403(R) (2014)

Analysis of the noise spectra from oxidized superparamagnetic nanoparticles

S. I. Woods,[1,*] Snorri Ingvarsson,[2] Shouheng Sun,[3] and J. R. Kirtley[4]

[1]*National Institute of Standards and Technology, 100 Bureau Drive, Gaithersburg, Maryland 20899, USA*

[2]*Science Institute, University of Iceland, Dunhaga 3, Reykjavik IS-107, Iceland*

[3]*Department of Chemistry, Brown University, Providence, Rhode Island 02912, USA*

[4]*Center for Probing the Nanoscale, Stanford University, Palo Alto, California 94305-4045, USA*

(Received 5 June 2014; revised manuscript received 12 June 2014; published 18 August 2014)

Expressions for the thermal noise from a collection of exchange-biased magnetic nanoparticles are derived and used to analyze the magnetic noise from thin films of partially oxidized nanoparticles. Functionalized Co nanoparticles with diameters between 3 and 6 nm were oxygenated in solution and then deposited on oxidized silicon substrates, self-assembling into arrays of magnetic nanoparticles during solvent evaporation. Magnetization measurements exhibited the development of exchange bias with oxygenation as evidenced by an increasing exchange field and coercivity. Noise measurements of the exchange-biased nanoparticles using a micro-superconducting quantum interference device sensor are shown to be consistent with theoretical expectations and are used to extract the magnetic energy distributions of the Co/CoO nanoparticles.

DOI: 10.1103/PhysRevB.90.060403 PACS number(s): 75.50.Tt, 05.40.Ca, 75.30.Et, 75.20.−g

A quantitative understanding of thermally driven magnetic fluctuations is critical to the study of magnetic nanoparticles. These nanoparticles exhibit superparamagnetism, or random spin flips induced by thermal energy, often at temperatures far below room temperature [1,2]. Although superparamagnetism is often a sign of nonideal behavior in materials designed to have fixed magnetic orientation such as magnetic memory, superparamagnetic signatures can be used to characterize and optimize nanoparticle systems. In particular, the random spin flips of magnetic nanoparticles generate a magnetic noise signature as a function of temperature which can be used to extract the magnetic anisotropy distribution of a population of nanoparticles [3,4]. Measuring the uniformity of magnetic distributions can be critical to the optimization of nanoparticle growth techniques for magnetic devices or materials under development for nanomedicine [5,6].

Superparamagnetism has been well studied for simple ferromagnetic nanoparticles [7–9], but there has been limited research of superparamagnetism in exchange-biased nanomagnetic systems [10]. In exchange-biased nanoparticle and thin-film systems, the magnetization of a ferromagnetic material can be uniaxially pinned by the exchange interaction with an antiferromagnetic material in intimate contact. The Co/CoO system is a model one for exchange bias and typically is characterized by changes in magnetization as a function of field and temperature [11–14]. Exchange-biased systems are technologically important for use in magnetoresistive devices and magnetic storage materials [15].

In this work, we extend a measurement method originally developed for the study of ferromagnetic nanoparticles to exchange-biased nanoparticles [4]. The method directly probes superparamagnetism by measuring the magnetic noise signal emanating from a two-dimensional array of self-assembled nanoparticles using a small superconducting quantum interference device (SQUID) sensor. In previous work, magnetic noise power as a function of temperature and frequency was used to extract magnetic anisotropy distributions of thin films of ferromagnetic particles, determining the magnetic uniformity of the nanoparticles under study. By taking into account how superparamagnetic noise is modified by exchange bias at the single particle level, it is possible to estimate the anisotropy distribution of a population of exchange-biased nanoparticles.

The noise power from a simple superparamagnetic particle has the form of a Markov process with a single time constant [16,17]. The magnetic noise power in this case has the form

$$S_B \propto \frac{\left(\frac{\tau}{2}\right)}{1+\omega^2\left(\frac{\tau}{2}\right)^2}, \tag{1}$$

where τ is the time constant for flipping of the particle moment and ω is the cyclic frequency of the measurement. The time constant has an activated form $\tau = \tau_0 \exp(U/k_B T)$, where U is the anisotropy energy of the particle, T is the temperature, and k_B is the Boltzmann constant. The noise power decreases with increasing frequency, often with a functional form near $1/\omega$ at low frequencies. The noise power as a function of temperature at a fixed frequency exhibits a curve with a single peak, which occurs at the temperature where the inverse flipping time is half the measurement frequency, i.e., $T_{\max} = -U/k_B \ln(\omega \frac{\tau_0}{2})$.

In the case of an exchange-biased superparamagnetic particle, there are different energies associated with the up and down spin directions, and the noise will depend, in general, on two time constants. Figure 1 contrasts the equal energy case of the simple superparamagnet with the unequal energy case associated with exchange bias, where an interaction with an antiferromagnet defines an energetically preferred direction, and the time constants σ and τ are associated with the two different spin directions. In the figure, the preferred direction is represented by the deeper "τ" well with energy $U_\tau > U_\sigma$ and time constant $\tau > \sigma$. The noise power generated by such a system with two distinct energies is nearly identical to that calculated by Machlup for the case of carrier trapping in semiconductors [16]. The magnetic noise power from a bistable, exchange-biased, single-domain particle with no interparticle interactions at temperature T, cyclic frequency

*Corresponding author: solomon.woods@nist.gov

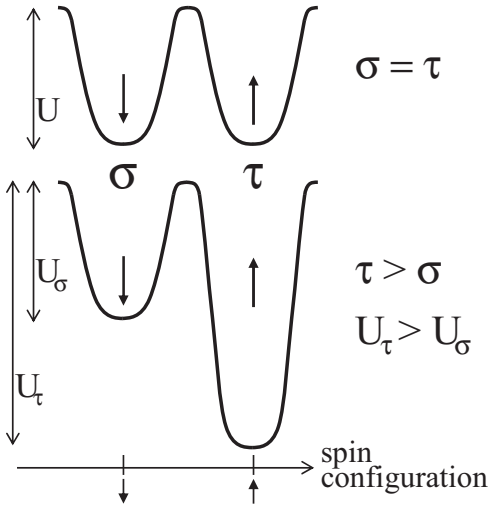

FIG. 1. Energy schematic contrasting the simple superparamagnetic (top) and exchange-biased (bottom) cases. A single energy and time constant are associated with both spin directions in the simple case, whereas exchange bias defines a preferred spin direction and results in a system with two distinct energies and two distinct time constants.

ω, and distance d away is

$$S_B(\omega,T) = \frac{4}{\pi}\left(\frac{\mu_0}{4\pi}\frac{MV}{d^3}\right)\frac{4\sigma\tau}{(\sigma+\tau)^2}\frac{\left(\frac{\tau_{\text{eff}}}{2}\right)}{1+\omega^2\left(\frac{\tau_{\text{eff}}}{2}\right)^2}, \quad (2)$$

where M is the particle magnetization, V is the particle volume, and $\tau_{\text{eff}} = 2(\frac{1}{\sigma}+\frac{1}{\tau})^{-1}$. Thus, the exchange bias case has noise power form similar to the simple superparamagnet where there is an effective flipping rate $1/\tau_{\text{eff}}$ which is equal to the average of the two flipping rates $1/\sigma$ and $1/\tau$, and there is an additional prefactor $4\sigma\tau/(\sigma+\tau)^2$.

There are two limits of interest: the case where the time constants are equal ($\sigma = \tau$) and the case where one time constant is much smaller than the other ($\sigma \ll \tau$). The $\sigma = \tau$ case is the simple superparamagnet limit and as expected Eq. (2) reduces to the form of Eq. (1). In the $\sigma \ll \tau$ case where one magnetization direction is much preferred over the other, Eq. (2) reduces to

$$S_B(\omega,T) \propto \frac{4}{\pi}\left(\frac{\sigma}{\tau}\right)\frac{\sigma}{1+\omega^2\sigma^2}, \quad (3)$$

which looks like the simple superparamagnetic form where the flipping time is twice that of the shallower well and there is an additional prefactor σ/τ.

The noise signal from a collection of particles will be a convolution of the single particle spectrum with the energy distribution of the population. For a distribution $\mathcal{D}(U)$ of particle anisotropy energies, the noise power of a population is $S_B^{\text{tot}} = \int_0^\infty S_B(U)\mathcal{D}(U)dU$, where $S_B(U)$ is the single particle noise power signal. If $\mathcal{D}(U)$ is expanded in a power series, then S_B^{tot} can be integrated term by term for the case of a simple superparamagnet to render [18,19]

$$S_B(\omega,T) \propto \frac{1}{\omega}\sum_{n=0}^{\infty}\frac{|E_{2n}|}{(2n)!}\left(\frac{\pi kT}{2}\right)^{2n+1}\mathcal{D}^{(2n)}(\tilde{U}), \quad (4)$$

where E_m is the mth Euler number and $\tilde{U} = -k_BT\ln(\omega\frac{\tau_0}{2})$. For $\mathcal{D}(U)$ slowly varying with respect to kT around $\tilde{U}$, the first term of the series is a good approximation and implies

$$\mathcal{D}(\tilde{U}) \propto \frac{2\omega}{\pi kT}S_B^{\text{tot}}. \quad (5)$$

As shown in earlier work [4], this expression can be used to approximate the distribution of anisotropy energies for a population of simple superparamagnets from its noise signal.

The noise signal from a population of exchange-biased magnetic particles depends on the distribution of both anisotropy energies and exchange energies, or equivalently the energies associated with the two wells in Fig. 1. For a distribution $\mathcal{D}(U_\tau,U_\sigma)$ of particle energies, in the case where $\sigma \ll \tau$, the total noise power can be written as follows:

$$S_B^{\text{tot}}(\omega,T) \propto \frac{\sigma_0}{\tau_0}\int_0^\infty\int_0^\infty e^{-\Delta U/kT}\frac{\sigma_0 e^{U_\sigma/kT}}{1+\omega^2\sigma_0^2e^{2U_\sigma/kT}} \times \mathcal{D}(U_\sigma,\Delta U)\,dU_\sigma d\Delta U, \quad (6)$$

where $\sigma = \sigma_0\exp(U_\sigma/kT)$ and $\Delta U = U_\tau - U_\sigma = 2MH_{ex}$ is the exchange energy. Expanding $\mathcal{D}(U_\sigma,\Delta U)$ in a power series about $(\tilde{U}_\sigma,\Delta\tilde{U})$ and retaining only the zeroth-order term, which is a good approximation for $\mathcal{D}(U_\sigma,\Delta U)$ slowly varying about $(\tilde{U}_\sigma,\Delta\tilde{U})$,

$$\begin{aligned} S_B^{\text{tot}}(\omega,T) &\propto \frac{\sigma_0}{\tau_0}\mathcal{D}(\tilde{U}_\sigma,\Delta\tilde{U})\left(\int_0^\infty e^{-\Delta U/kT}d\Delta U\right) \\ &\quad\times\left(\int_0^\infty\frac{\sigma_0e^{U_\sigma/kT}}{1+\omega^2\sigma_0^2e^{2U_\sigma/kT}}dU_\sigma\right) \\ &\propto \mathcal{D}(\tilde{U}_\sigma,\Delta\tilde{U})\frac{\pi kT}{2\omega}kT. \end{aligned} \quad (7)$$

In contrast to the case of the simple superparamagnet, it can be seen that this zeroth-order term is quadratic in kT rather than linear. Higher orders of $\mathcal{D}(U_\sigma,\Delta U)$ can be retained if one assumes $\mathcal{D}$ is separable in U_σ and ΔU, that $\mathcal{D}$ has a broad Gaussian shape in ΔU, and is slowly varying with respect to kT, in which case

$$\begin{aligned} S_B^{\text{tot}}(\omega,T) &\propto \left[\frac{1}{\omega}\sum_{n=0}^{\infty}\frac{|E_{2n}|}{(2n)!}\left(\frac{\pi kT}{2}\right)^{2n+1}\mathcal{D}^{(2n)}(\tilde{U}_\sigma)\right] \\ &\quad\times\left[\left(1-\frac{(\Delta\tilde{U})^2}{s^2}\right)kT+\frac{2\Delta\tilde{U}}{s^2}(kT)^2 \right. \\ &\quad\left.-\frac{2}{s^2}(kT)^3+\cdots\right], \end{aligned} \quad (8)$$

where $\mathcal{D}(\Delta\tilde{U}) \propto \exp(\frac{-(\Delta U-\Delta\tilde{U})^2}{s^2})$ and $s \gg \Delta\tilde{U} \geqslant kT$.

The samples were thin films of self-assembling Co and Co/CoO nanoparticles deposited on thermally oxidized silicon substrates. Monodisperse cobalt nanoparticles with the multiply twinned face-centered cubic (mt-fcc) or ε-Co structure were fabricated using high temperature solution phase synthesis, coated with oleate, dispersed in hexane or dodecane, and deposited on substrates where they self-assembled into close-packed arrays as the solvent evaporated [20]. Exchange-biased samples began as monodisperse Co nanoparticles with diameters of 3 or 6 nm and were partially oxidized either by

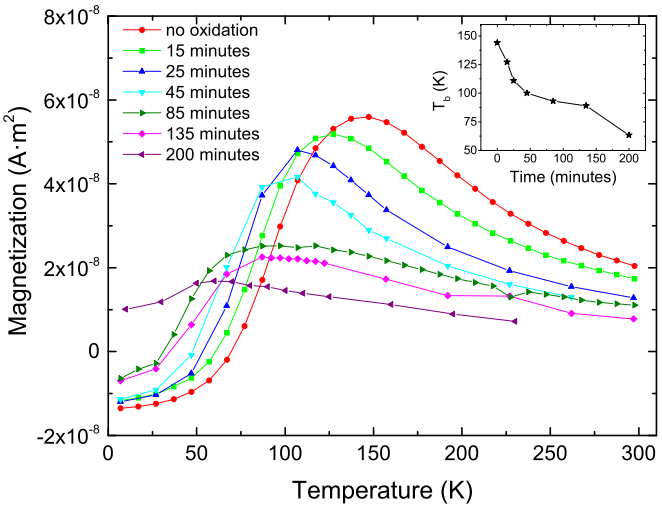

FIG. 2. (Color online) Magnetization as a function of temperature for a series of 6-nm ε-Co samples oxygenated in heated solution for different periods of time. The data exhibits ZFC curves, and shows that blocking temperature falls monotonically with increasing oxygenation time. The inset plot shows the peak temperature of the M-T curves as a function of oxygenation time.

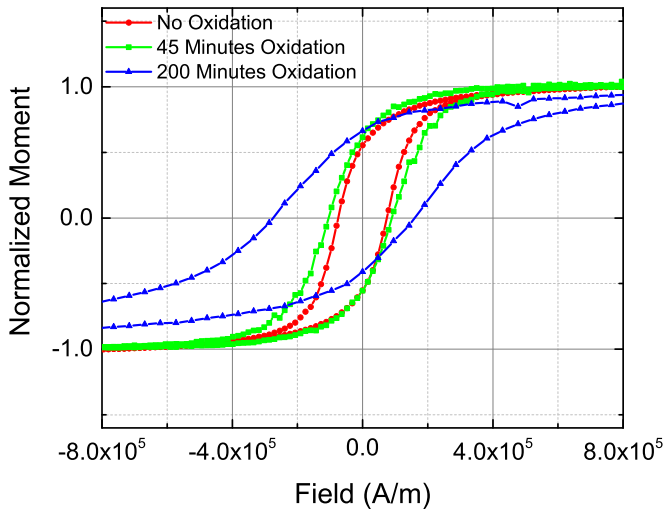

FIG. 3. (Color online) FC M-H curves for 6 nm ε-Co samples oxygenated 0, 45, and 200 minutes. Coercivity and exchange field increase with oxygenation.

aging in atmosphere or bubbling oxygen through a dodecane dispersion at 100 °C.

Magnetization measurements of the samples as a function of temperature and applied field were made using a Quantum Magnetics MPMS system [21]. Zero-field-cooled (ZFC) magnetization-temperature (M-T) measurements were made by cooling from 300 K in zero field and warming in a 795.8 A/m (10 Oe) field, providing a value for blocking temperature. ZFC and field-cooled (FC) magnetization-field (M-H) measurements were acquired, cooling from 300 to 5 K in zero field (ZFC) or 4 T (FC) before scanning through a range of applied fields. Noise measurements were made using a variable temperature scanning SQUID microscope with a niobium SQUID which had a square pickup loop 17.8 μm on a side [22]. The output from the SQUID electronics was analyzed using an HP35665A digital signal analyzer [21] to study the magnetic noise of the nanoparticles at frequencies from 10 to 10 000 Hz and sample temperatures from 4 to 100 K. The SQUID could be scanned in near contact with the nanoparticles ($\sim$3 μm away) and at heights of 100–500 μm, allowing background signals and frequency response of the SQUID to be separated from the sample signal.

A number of nominally identical 6 nm ε-Co samples were oxygenated in dodecane solution for varying amounts of time between 0 and 200 minutes. These samples exhibited blocking temperatures (T_b) between 140 and 65 K, as shown by the ZFC curves in Fig. 2, T_b falling monotonically with increasing oxygenation time. The standard uncertainty for any datapoint in Fig. 2 is less than 1.2×10^{-9} A/m, and the mean standard uncertainty over temperatures for any curve is less than 2.0×10^{-10} A/m. As more CoO forms with longer oxygenation time, the volume of the ferromagnetic core decreases. Similarly, a 3-nm mt-fcc Co sample oxygenated by aging in atmosphere exhibited a drop in blocking temperature from 12 to 5 K. The series of 6-nm ε-Co samples shows increasing coercivity and increasing field offset in the FC data with increasing oxygenation time. The increasing coercivity and field offset are evidence of exchange bias and demonstrate development of an exchange field with oxygenation of the Co nanoparticles. Figure 3 shows the field-cooled M-H data for three of the 6-nm ε-Co samples, oxygenated for 0, 45, and 200 minutes. Coercivity increases from 7.44×10^4 A/m (935 Oe) to 2.18×10^5 A/m (2734 Oe) over the series and field offset increases from 127 A/m (1.6 Oe) to 5.70×10^4 A/m (716 Oe). For each of the curves in Fig. 3, the mean standard uncertainty of the magnetization values is less than 0.8% of the saturation magnetization.

Magnetic noise power as a function of temperature is shown for the partially oxidized 3 nm mt-fcc Co sample at three frequencies in Fig. 4. The average noise power floor for this data is less than 1.2×10^{-22} T^2/Hz. As for simple superparamagnetic nanoparticles, the temperature-dependent noise power curves exhibit a single peak, and as seen in Fig. 4 the location of the peak moves to higher temperature with increasing measurement frequency.

The magnetic noise power data as a function of frequency and temperature was used to derive estimates for the anisotropy energy distributions of exchange-biased samples. If the exchange energy is relatively small and the two time constants are approximately equal ($\sigma \approx \tau$), then the noise is that of a simple superparamagnet and to lowest order the energy distribution can be found from Eq. (5). If the exchange energy is large enough that the two time constants are significantly different ($\sigma \ll \tau$), then the energy distribution can be found from Eq. (7). When the appropriate relation is chosen for a particular sample, all the transformed data should define a single common energy distribution curve for the sample. The peak anisotropy energy $\tilde{U}$ ($\tilde{U}_\sigma$) is given by $-k_B T \ln(\omega \frac{\tau_0}{2})$ [$-k_B T \ln(\omega\sigma_0)$] for the simple (exchange-biased) case. Plotting the transformed magnetic noise data [transformed to an energy distribution using Eqs. (5) or (7)] against the peak anisotropy energy $\tilde{U}$, it was found that a well-defined energy distribution was followed by the oxidized 3 nm mt-fcc Co when Eq. (5) was used, but

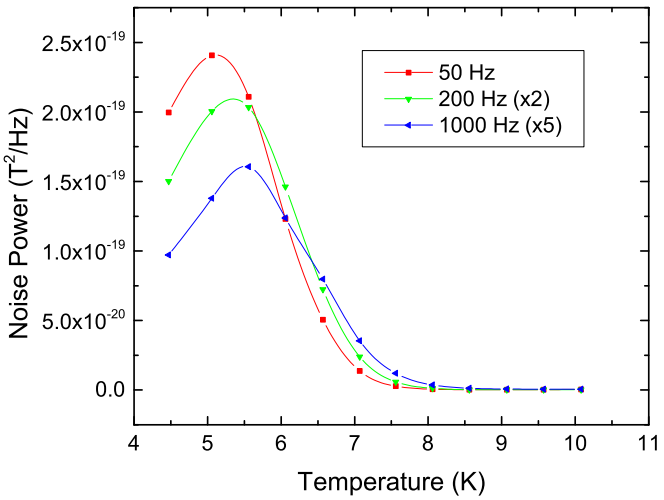

FIG. 4. (Color online) Magnetic noise power as a function of temperature at different measurement frequencies for a thin film of partially oxidized 3-nm mt-fcc Co nanoparticles. The curves exhibit a single peak in temperature which moves out to higher temperatures with increasing frequency.

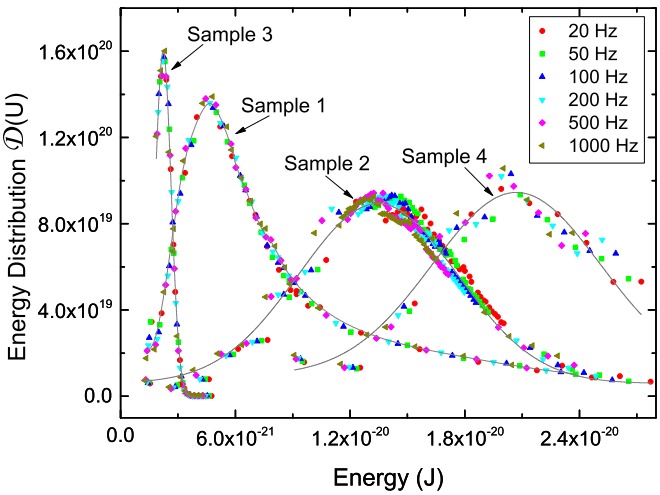

FIG. 5. (Color online) Calculated magnetic energy distributions of nonoxidized 3 nm mt-fcc Co (sample 1), and partially oxidized 3 nm mt-fcc Co (sample 3); calculated magnetic energy distributions of nonoxidized 5 nm mt-fcc Co (sample 2) and partially oxidized (200 minutes oxygenation) 6 nm ε-Co (sample 4). Temperature-dependent magnetic noise data at the fixed frequencies listed in the legends were used to calculate each energy distribution.

that Eq. (7) yielded a distribution curve with less scatter for the oxidized (200 min. oxygenation) 6 nm ε-Co.

Figure 5 shows the energy distribution calculated for the 3 nm (sample 3) and 6 nm (sample 4) oxidized samples, as well as the energy distributions calculated using Eq. (5) for two nonoxidized simple superparamagnetic mt-fcc Co samples with nanoparticle diameters of 3 nm (sample 1) and 5 nm (sample 2) for comparison. The partially oxidized 3-nm sample exhibits a lower peak energy than the nonoxidized 3-nm sample and less of a high-energy tail. The oxidized 6-nm particles have an energy distribution about the same width as the nonoxidized 5-nm particles and both samples have been approximately fit by Gaussian distributions as guides to the eye. For the exchange-biased 6-nm ε-Co particles it is not possible to determine how the distribution separately depends upon anisotropy and exchange energy, but the assumption has been made that the exchange energy distribution is approximately flat about an energy defined by the field shift measured in the M-H data. Thus the distribution calculated from Eq. (7) for this sample is identified as the anisotropy energy distribution, but has been shifted by an exchange energy of approximately 6.65×10^{-21} J.

We have derived expressions for the thermally driven magnetic noise produced by a population of exchange-biased magnetic nanoparticles. The noise power signal from a single nanoparticle depends upon two different flipping time constants because exchange bias defines a preferred moment direction, but the expression for noise power is similar to that for a simple superparamagnet where the effective time constant is the average of the two flipping time constants. In the case where one time constant is much smaller than the other, the effective time constant is twice the smaller time constant. Analysis predicts that for weak exchange bias, the magnetic energy distribution for a population of nanoparticles is proportional to $\frac{\omega}{kT} S_B^{\mathrm{tot}}(\omega, T)$ in lowest order, whereas for strong exchange bias, the distribution is proportional to $\frac{\omega}{(kT)^2} S_B^{\mathrm{tot}}(\omega, T)$. Experimentally, we have demonstrated that exchange bias can be introduced into thin-film arrays of magnetic nanoparticles by oxygenating them in heated solution before deposition. With appropriate assumptions, consistent magnetic energy distributions were determined for oxygenated 3-nm mt-fcc Co and 6-nm ε-Co samples from temperature- and frequency-dependent magnetic noise data. Partial oxygenation, as well as overall particle size, can be used to tune the location of the peak in the temperature-dependent noise of nanoparticle samples. For monodisperse samples this peak in temperature can be rather sharp, and so nanoparticle samples could find application as noise thermometers tuned for sensitivity at temperatures of interest.

This experiment was inspired by discussions with R. H. Koch, who first suggested to one of the authors (S.W.) the similarity between magnetic noise in the exchange-biased system and the current noise in semiconductors described by Machlup. All sample preparation and data collection for this experiment were conducted at the IBM T.J. Watson Research Center in Yorktown Heights, NY when the authors were researchers there.

[1] C. P. Bean and J. D. Livingston, J. Appl. Phys. **30**, S120 (1959).

[2] William T. Coffey and Yuri P. Kalmykov, J. Appl. Phys. **112**, 121301 (2012).

[3] T. Jonsson, P. Nordblad, and P. Svedlindh, Phys. Rev. B **57**, 497 (1998).

[4] S. I. Woods, J. R. Kirtley, Shouheng Sun, and R. H. Koch, Phys. Rev. Lett. **87**, 137205 (2001).

[5] S. Sun, C. B. Murray, D. Weller, L. Folks, and A. Moser, Science **287**, 1989 (2000).
[6] L. Zhang, F. X. Gu, J. M. Cha, A. Z. Wang, R. S. Langer, and O. C. Farokhzad, Clin. Pharmacol. Ther. (NY) **83**, 761 (2008).
[7] C. Petit and M. P. Pileni, Appl. Surf. Sci. **162-163**, 519 (2000).
[8] J. van Lierop and D. H. Ryan, Phys. Rev. Lett. **85**, 3021 (2000).
[9] T. Jonsson, J. Mattsson, P. Nordblad, and P. Svedlindh, J. Magn. Magn. Mater. **168**, 269 (1997).
[10] Vassil Skumryev, Stoyan Stoyanov, Yong Zhang, George Hadjipanayis, Dominique Givord, and Josep Nogues, Nature (London) **423**, 850 (2003).
[11] W. H. Meiklejohn and C. P. Bean, Phys. Rev. **105**, 904 (1957).
[12] D. L. Peng, K. Sumiyama, T. Hihara, S. Yamamuro, and T. J. Konno, Phys. Rev. B **61**, 3103 (2000).
[13] F. T. Parker, Kentaro Takano, and A. E. Berkowitz, Phys. Rev. B **61**, R866 (2000).
[14] Qin-tang Wang, Guo-hong Pan, and Yun-xi Sun, J. Magn. Magn. Mater. **78**, 190 (1989).
[15] J. Nogues and Ivan K. Schuller, J. Magn. Magn. Mater. **192**, 203 (1999).
[16] Stefan Machlup, J. Appl. Phys. **25**, 341 (1954).
[17] M. J. Buckingham, *Noise in Electronic Devices and Systems* (Ellis Horwood Limited, New York, 1983), p. 33.
[18] I. S. Gradshteyn and I. M. Ryzhik, *Table of Integrals, Series, and Products* (Academic Press, New York, 1980), p. 349.
[19] P. Dutta, P. Dimon, and P. M. Horn, Phys. Rev. Lett. **43**, 646 (1979).
[20] S. Sun and C. B. Murray, J. Appl. Phys. **85**, 4325 (1999).
[21] Reference is made to commercial products to adequately specify the experimental procedures involved. Such identification does not imply recommendation or endorsement by the National Institute of Standards and Technology, nor does it imply that these products are the best for the purpose specified.
[22] J. R. Kirtley, C. C. Tsuei, K. A. Moler, V. G. Kogan, J. R. Clem, and A. J. Turberfield, Appl. Phys. Lett. **74**, 4011 (1999).